Scientific Research Publishing

World Journal of Condensed Matter Physics, 2023, 13, 40-56
https://www.scirp.org/journal/wjcmp
ISSN Online: 2160-6927
ISSN Print: 2160-6919

AC Back Surface Recombination Velocity as Applied to Optimize the Base Thickness under Temperature of an (n^+-p-p^+) Bifacial Silicon Solar Cell, Back Illuminated by a Light with Long Wavelength

Khady Loum[1,2], Ousmane Sow[1,2], Gora Diop[1,2], Richard Mane[1], Ibrahima Diatta[1], Malick Ndiaye[1], Sega Gueye[1], Moustapha Thiame[1,3], Mamadou Wade[1,4], Gregoire Sissoko[1]

[1]International Research Group in Renewable Energy (GIRER), Dakar, Sénégal
[2]Institut Universitaire de Technologie, Université Iba Der THIAM de Thiès, Thiès, Senegal
[3]Université Assane SECK, Ziguinchor, Senegal
[4]Ecole Polytechnique de Thiès, Thiès, Senegal
Email: gsissoko@yahoo.com

How to cite this paper: Loum, K., Sow, O., Diop, G., Mane, R., Diatta, I., Ndiaye, M., Gueye, S., Thiame, M., Wade, M. and Sissoko, G. (2023) AC Back Surface Recombination Velocity as Applied to Optimize the Base Thickness under Temperature of an (n^+-p-p^+) Bifacial Silicon Solar Cell, Back Illuminated by a Light with Long Wavelength. *World Journal of Condensed Matter Physics*, **13**, 40-56.
https://doi.org/10.4236/wjcmp.2023.131003

Received: November 12, 2022
Accepted: February 25, 2023
Published: February 28, 2023

Abstract

The bifacial silicon solar cell, placed at temperature (T) and illuminated from the back side by monochromatic light in frequency modulation (ω), is studied from the frequency dynamic diffusion equation, relative to the density of excess minority carriers in the base. The expressions of the dynamic recombination velocities of the minority carriers on the rear side of the base $Sb1(D(\omega, T); H)$ and $Sb2(\alpha, D(\omega, T); H)$, are analyzed as a function of the dynamic diffusion coefficient ($D(\omega, T)$), the absorption coefficient ($\alpha(\lambda)$) and the thickness of the base (H). Thus their graphic representation makes it possible to go up, to the base optimum thickness ($Hopt(\omega, T)$), for different temperature values and frequency ranges of modulation of monochromatic light, of strong penetration. The base optimum thickness ($Hopt(\omega, T)$) decreases with temperature, regardless of the frequency range and allows the realization of the solar cell with few material (Si).

Keywords

Bifacial Silicon Solar Cell, Absorption Coefficient, Frequency, Temperature, Recombination Velocity, Optimum Thickness

1. Introduction

This work aims to determine the optimum thickness of the base [1] [2] [3] of the bifacial silicon solar cell ($n^+/p/p^+$) [4] [5] [6] [7] [8]. The base (p) of the bifacial silicon solar cell ($n^+/p/p^+$) maintained at temperature (T), is studied under monochromatic illumination (λ) in frequency modulation (ω).

The monochromatic light chosen, induces an absorption coefficient ($\alpha(\lambda)$ = 6.02 cm^{-1}) [9] [10] and penetrates deep into the silicon material. The frequency dynamic diffusion equation relating to the density of the excess charge minority carriers in the base of the solar cell is solved. The boundaries of this zone, which are the junction (n^+/p) in $x = 0$ and the rear face (p/p^+) in $x = H$, impose conditions that use the recombination velocities of minority carriers, respectively (Sf) [11] [12] [13] [14] [15] and (Sb) [16]-[24]. Taking into account the dynamic diffusion coefficient ($D(\omega, T)$) related to the temperature (T) [25] [26] [27] and the frequency (ω) of modulation [28]-[33], as well as the recombination velocities (Sf) at the junction and (Sb) at the rear side, the expression of the dynamic photocurrent density of the minority charge carriers $Jph(Sf, Sb, \alpha, H, D(\omega, T))$ is established and represented graphically as a function of (Sf), for different temperatures and frequency zones.

From this representation, the expressions $Sb(\alpha, H, D(\omega, T))$ and $Sb(H, D(\omega, T))$ of the dynamic rate of recombination of the minority charge carriers on the rear side of the base, are deduced. The graphic technique of representation [34]-[44] of these expressions as a function of the base thickness (H), makes it possible to determine the optimum thickness ($Hopt$), for given temperature values and for different frequency zones. The optimum thickness ($Hopt(T)$) is represented by curves as function of temperature, for each frequency range studied.

The modeling analysis of these curves, through the effects of temperature (thermal agitation), frequency (relaxation time) and a low absorption coefficient (deep penetration), shows the possibility of developing the bifacial solar cell by a reduction in thickness, according to the conditions of use while producing an optimal photocurrent.

2. Theory

The structure of the n^+-p-p^+ bifacial silicon solar cell at (T) temperature and back illuminated with monochromatic light in frequency, is represented by **Figure 1**.

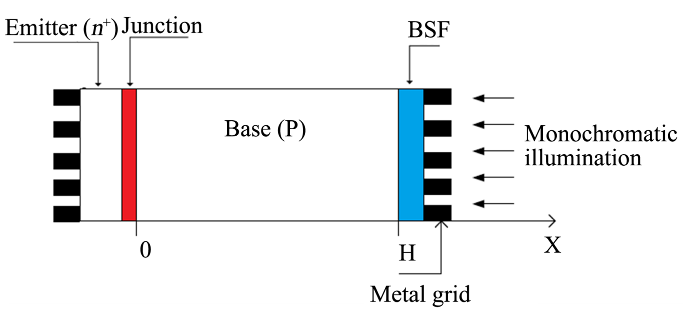

Figure 1. Schematic drawing of bifacial solar cell structure AC back illuminated.

The excess minority carriers' density $\delta(x, t)$ generated in the base of the solar cell, under monochromatic illumination, is governed by the following continuity equation [31] [32] [33]:

$$D(\omega,T)\times\frac{\partial^2\delta(x,t)}{\partial x^2}-\frac{\delta(x,t)}{\tau}=-G(x,\omega,t)+\frac{\partial\delta(x,t)}{\partial t} \quad (1)$$

The expression of the excess minority carriers' density is written, according to the space coordinates (x) and the time t, as:

$$\delta(x,t)=\delta(x)\cdot \mathrm{e}^{-j\omega t} \quad (2)$$

Ac Carrier generation rate $G(x, t)$ is given by the relationship:

$$G(x,t)=g(x)\cdot \mathrm{e}^{-j\omega t} \quad (3)$$

With:

$$g(x)=\alpha(\lambda)\cdot I_0(\lambda)\cdot\left(1-R(\lambda)\right)\cdot \mathrm{e}^{-\alpha(\lambda)\cdot(H-x)} \quad (4)$$

I_0 is the incident photon flux on the rear (p^+), at the solar cell base depth ($x = H$), while $\alpha(\lambda)$ and $R(\lambda)$ are respectively the optical [9] [10] absorption and reflection coefficients of Si material $D(\omega, t)$ is the complex diffusion coefficient of excess minority carrier in the base under T temperature. Its expression is given by the relationship [22] [23] [31] [32] [33]:

$$D(\omega,T)=D(T)\times\left(\frac{1-j\cdot\omega^2\cdot\tau^2}{1+(\omega\tau)^2}\right) \quad (5)$$

$D(T)$ is the temperature-dependent diffusion coefficient given by Einstein's relationship

$$D(T)=\frac{\mu(T)\cdot K_b\cdot T}{q} \quad (6)$$

T is the temperature in Kelvin, K_b is the Boltzmann constant:

$$K_b=1.38\times10^{-23}\ \mathrm{m}^2\cdot\mathrm{Kg}\cdot\mathrm{S}^{-1}\cdot\mathrm{K}^{-1}$$

The mobility coefficient [25] [26] [45] for electrons $\mu(T)$, is expressed according to the temperature and is given by:

$$\mu(T)=1.43\times10^{19}T^{-2.42} \quad (7)$$

By replacing **Equations (2) and (3)** in **Equation (1)**, the continuity equation for the excess minority carriers' density in the base is reduced to the following relationship:

$$\frac{\partial^2\delta(x)}{\partial x^2}-\frac{\delta(x)}{L^2(\omega,T)}=-\frac{g(x)}{D(\omega,T)} \quad (8)$$

$L(\omega, T)$ is the complex diffusion length of excess minority carriers' in the base given by:

$$L(\omega,T)=\sqrt{\frac{D(\omega,T)\tau}{1+j\omega\tau}} \quad (9)$$

The solution is expressed as following:

$$\delta(x,\lambda,\omega,T) = A\cdot\cosh\left[\frac{x}{L(\omega,T)}\right] + B\cdot\sinh\left[\frac{x}{L(\omega,T)}\right] + K\cdot e^{-\alpha(\lambda)\cdot(H-x)} \quad (10)$$

With:

$$K = -\frac{\alpha(\lambda)\cdot I_0\cdot(1-R)\cdot\left[L(\omega,T)\right]^2}{D(\omega,T)\left[L(\omega,T)^2\cdot\alpha(\lambda)^2-1\right]} \text{ and } \left(L(\omega,T)^2\cdot\alpha(\lambda)^2\neq 1\right) \quad (11)$$

Coefficients A and B are determined through the boundary conditions:

- At the junction ($x = 0$)

$$\left.\frac{\partial\delta(x,\lambda,\omega,T)}{\partial x}\right|_{x=0} = Sf\cdot\left.\frac{\delta(x,\lambda,\omega,T)}{D(\omega,T)}\right|_{x=0} \quad (12)$$

- On the back side in the base ($x = H$)

$$\left.\frac{\partial\delta(x,\lambda,\omega,T)}{\partial x}\right|_{x=H} = -Sb\cdot\left.\frac{\delta(x,\lambda,\omega,T)}{D(\omega,T)}\right|_{x=H} \quad (13)$$

(Sf) and (Sb) are respectively the recombination velocities of the excess minority carriers [46] at the junction and at the back surface. The recombination velocity Sf is imposed by the external load which fixes the solar cell operating point [11] [12] [47] [48] [49] [50]**.** At low value, it becomes intrinsic component which represents the carrier losses associated with the shunt resistor in the solar cell electrical equivalent model under open circuit operation [7] [15] [50]. The minority carrier recombination velocity (Sb) on the back surface is the consequence of the electric field created by the junction (p/p^+) which rejects the carrier toward the junction (n^+/p) [51] [52].

3. Results and Discussions

3.1. Ac Diffusion Coefficient and Frequency Domains

Previous works [18] [19] [29] [30] [53] [54] [55] have shown that the dynamic diffusion coefficient of minority carriers in the base of the solar cell is of constant amplitude at low frequencies (steady state: $\omega < \omega_c$, ω_c is the cut-off frequency) and it decreases at high frequencies (dynamic regime: $\omega < \omega_c$). The amplitude of the diffusion coefficient of minority carriers decreases very rapidly with frequency. The higher the frequency, the lower the relaxation time of the minority carriers, then this produces as a consequence a greater probability of recombination of minority carriers, hence the drastic decrease of the diffusion coefficient, which corresponds to the third frequency interval. For the rest of the study, three frequencies from these intervals will be taken into account.

3.2. Photocurrent

Ac photocurrent density at the junction is obtained from ac minority carriers' density in the base and $\delta(x, Sf, Sb, H, \omega, T, \alpha(\lambda))$ is given by the following expression:

$$J_{ph}\left(Sf,Sb,H,\omega,T,\alpha\left(\lambda\right)\right)=qD\left(\omega,T\right)\left.\frac{\partial\delta\left(x,Sf,Sb,H,\omega,T,\alpha\left(\lambda\right)\right)}{\partial x}\right|_{x=0} \tag{14}$$

where q is the elementary electron charge.

Figures 2-4 show ac photocurrent versus junction surface recombination velocity respectively, for different frequency values ($\omega = 10^3$ rad·s^{-1}, $\omega = 10^5$ rad·s^{-1}, $\omega = 10^6$ rad·s^{-1}).

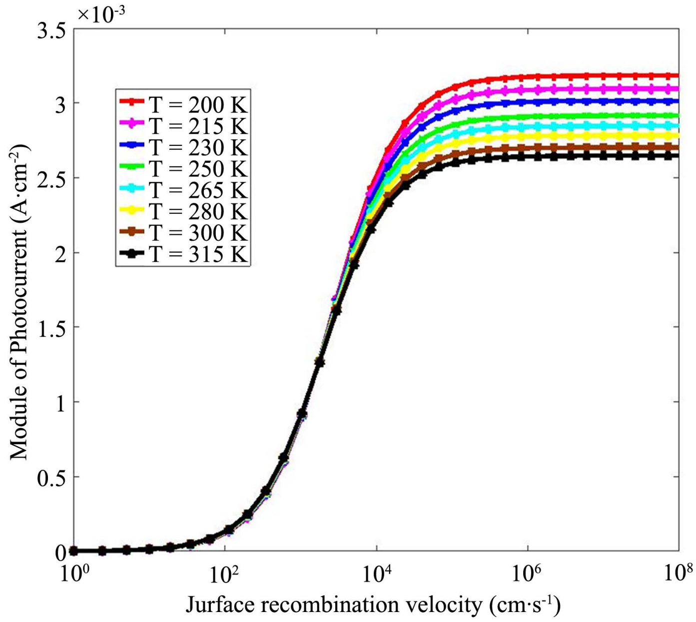

Figure 2. Module of Ac photocurrent density versus junction recombination velocity for different diffusion coefficient values ($\omega = 10^3$ rad·s^{-1}; $\alpha = 6.2$ cm^{-1}).

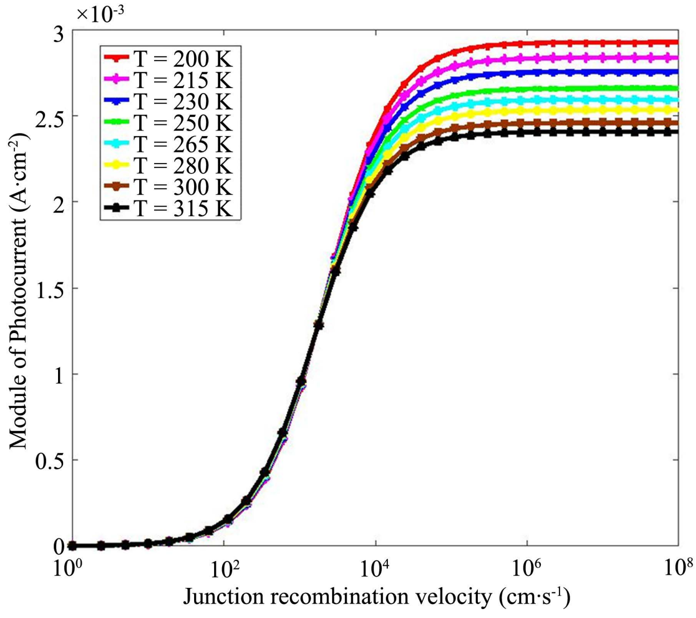

Figure 3. Module of ac photocurrent density versus junction recombination velocity for different diffusion coefficient values ($\omega = 10^5$ rad·s^{-1}; $\alpha = 6.2$ cm^{-1}).

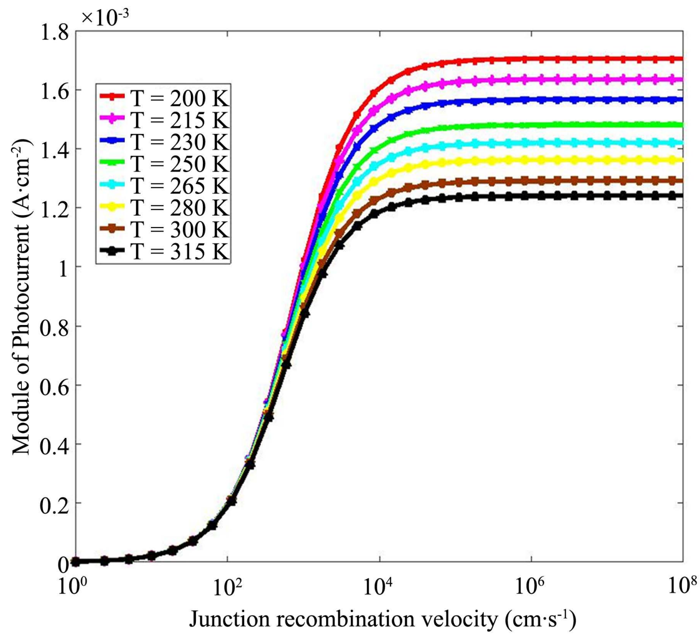

Figure 4. Module of ac photocurrent density versus junction recombination velocity for different diffusion coefficient values ($\omega = 10^6$ rad·s^{-1}; $\alpha = 6.2$ cm^{-1}).

The amplitude of the density of the dynamic photocurrent (J_{ph}), as function of the recombination rate (Sf) at the junction, for different temperature values, is represented by the **Figures 2-4**, corresponding to the three frequency domains, shows three zones. At low values of (Sf), the amplitude of the photocurrent density is zero, regardless of temperature, for the three frequency domains and corresponds to the open circuit operation of the solar cell. The amplitude of the photocurrent density increases rapidly with (Sf), and reaches an asymptotic value corresponding to the short-circuit operation of the solar cell. The amplitude of the short-circuit photocurrent density ($J_{ph,sc}$) decreases with temperature and frequency. Indeed, the density profile of minority carriers at depth in the base of the short-circuited solar cell is modified with temperature (amplitude reduction) [56] and with frequency (by reducing the relaxation time) [18] [19] [20] [21] [29] [30] as suggested throughout **Equations (5), (6) and (9)**.

3.3. Back Surface Recombination Velocity Determination and Base Thickness Optimization with Both, Temperature and Frequency

The plot of ac photocurrent density amplitude versus minority carriers' recombination velocity at the junction shows a bearing sets up, for very large Sf, and corresponds to short-circuit current density (J_{phsc}). Then in this zone, we can write [12] [13] [14] [55]:

$$\left.\frac{\partial J_{ph}\left(Sf, Sb, H, \omega, T, \alpha(\lambda)\right)}{\partial Sf}\right|_{Sf \geq 10^5\ \mathrm{cm \cdot s^{-1}}} = 0 \tag{15}$$

The solution of Equation (15) leads to the ac recombination velocity in the back surface expressions given by Equations (16) and (17):

$$Sb1(\omega,H,T) = -\frac{D(\omega,T)}{L(\omega,T)} \cdot \tanh\left(\frac{H}{L(\omega,T)}\right) \quad (16)$$

$$Sb2(\omega,H,T,\lambda) = \frac{D(\omega,T)}{L(\omega,T)} \cdot \left[\frac{\alpha(\lambda)\cdot L(\omega,T) - \left(\sinh\left(\frac{H}{L(\omega,T)}\right) + \alpha(\lambda)\cdot L(\omega,T)\cdot\cosh\left(\frac{H}{L(\omega,T)}\right)\right)\exp(-\alpha(\lambda)\cdot H)}{\exp(-\alpha(\lambda)\cdot H)\cdot\left(\cosh\left(\frac{H}{L(\omega,T)}\right) + \alpha(\lambda)\cdot L(\omega,T)\cdot\sinh\left(\frac{H}{L(\omega,T)}\right)\right) - 1}\right] \quad (17)$$

Figures 5-7 representation two expressions of back surface recombination velocity versus solar cell base thickness, for different temperature values, respectively in the three frequency domains. **Tables 1-3**, give the results obtained, for the solar cell base optimum thickness again temperature, in the three frequency domains.

The optimum thickness is extracted from **Figure 4**, **Figure 5** and **Figure 9** for given temperatures and for the three frequency domains. The results are presented in the **Tables 1-3**.

Deduced from **Tables 1-3**, **Figure 8** and **Figure 9** are respectively the plots of Hopt again temperature and diffusion coefficient for frequency domains.

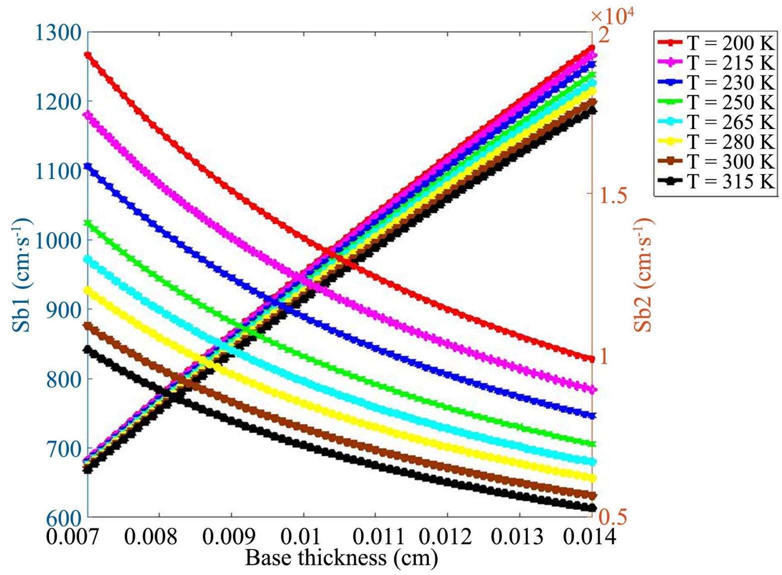

Figure 5. *Sb*1 and *Sb*2 versus base thickness for different values of the temperature (ω = 10^3 rad·s^{-1}; α = 6.2 cm^{-1}).

Table 1. Optimum thickness obtained, for different temperatures and for the frequency range (ω = 10^3 rad·s^{-1}).

T (K)	200	215	230	250	265	280	300	315
D (cm²/s)	66.65	60.14	54.65	48.55	44.69	41.33	37.48	34.97
Hop (cm)	0.0108	0.0104	0.0101	0.0098	0.0094	0.0092	0.0089	0.0086

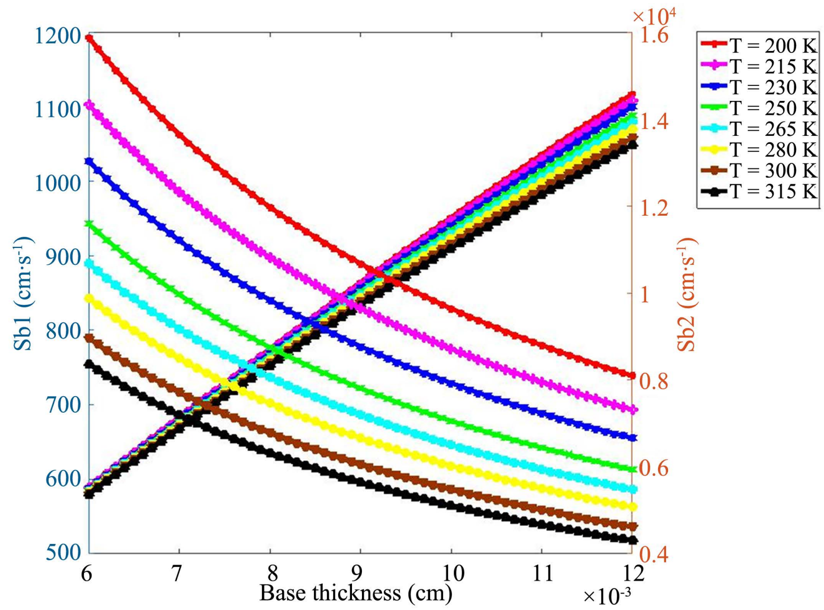

Figure 6. *Sb*1 and *Sb*2 versus base thickness for different values of the temperature (ω = 105 rad·s^{-1}; α = 6.2 cm^{-1}).

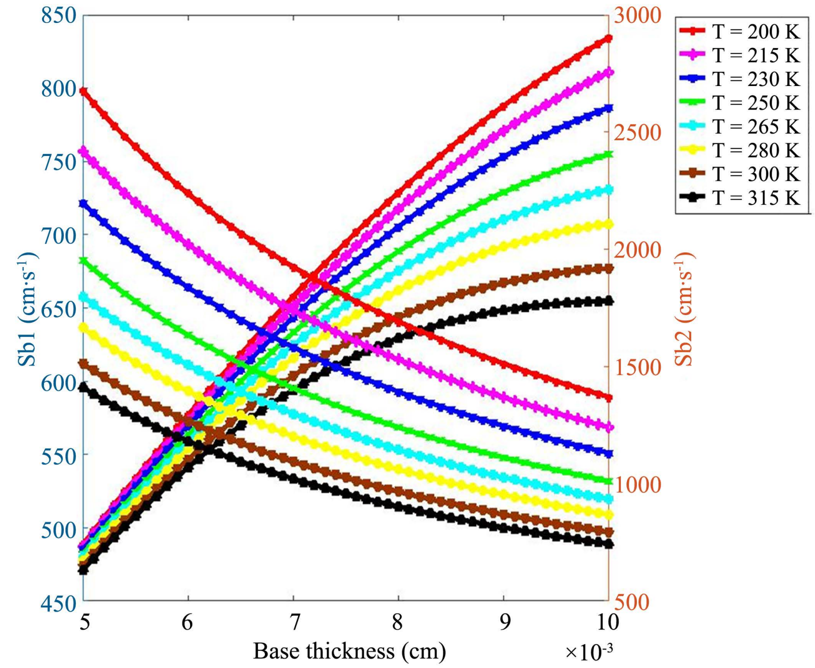

Figure 7. *Sb*1 and *Sb*2 versus base thickness for different values of the temperature (ω = 10^6 rad·s^{-1}; α = 6.2 cm^{-1}).

Table 2. Optimum thickness obtained, for different temperatures and for the frequency range (ω = 10^5 rad·s^{-1}).

T (K)	200	215	230	250	265	280	300	315
D (cm^2/s)	33.3278	30.0751	27.3285	24.2770	22.3491	20.6683	18.7395	17.4851
Hop (cm)	0.0089	0.0086	0.0083	0.0080	0.0078	0.0076	0.0074	0.0072

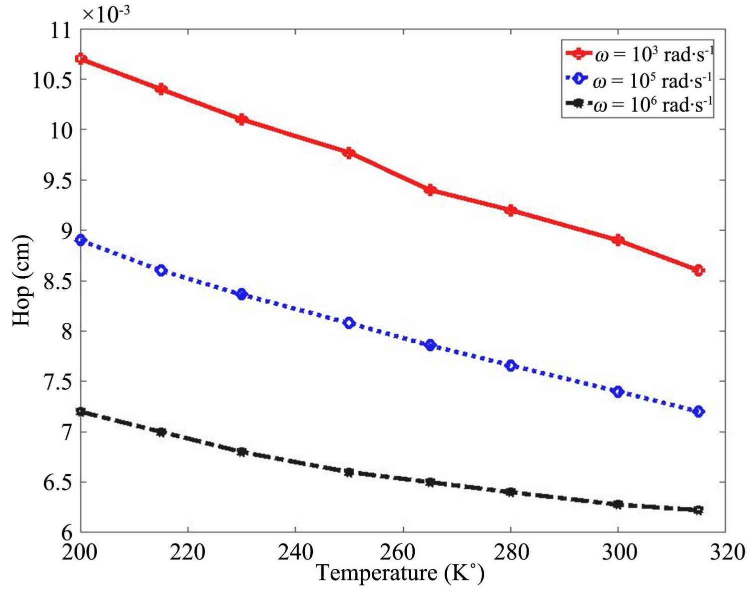

Figure 8. Optimum thickness versus temperature for different frequency values.

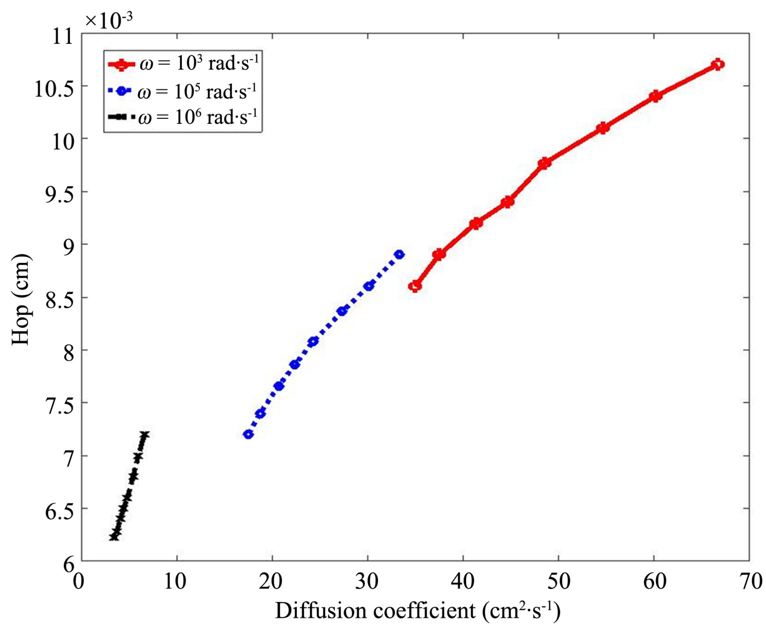

Figure 9. Optimum thickness versus diffusion coefficient for different frequency values.

Table 3. Optimum thickness obtained, for different temperatures and for the frequency range ($\omega = 10^6$ rad·s^{-1}).

T (K)	200	215	230	250	265	280	300	315
D(cm^2/s)	6.63	5.98	5.44	4.83	4.45	4.11	3.73	3.48
Hop (cm)	0.0072	0.007	0.0068	0.0066	0.0065	0.0064	0.0063	0.0062

4. Discussions

The modeling of the curves gave the mathematical correlations of the optimum thickness of the base *Hopt*(*T*) and *Hopt*(*D*), respectively as a function of the temperature (**Figure 8**) and the diffusion coefficient of the minority carriers of the base (**Figure 9**), according to the three frequency regimes:

1) Frequency regime: $\omega \le 10^3$ rad/s

$$Hop(cm)(T) = -1.8\times10^{-5}\times T + 0.014 \tag{18}$$

$$Hop(cm)(D) = 6.9\times10^{-5}\times D + 0.0063 \tag{19}$$

2) Frequency regime: 10^3 rad/s $< \omega \le 10^5$ rad/s

$$Hop(cm)(T) = -1.4\times10^{-5}\times T + 0.012 \tag{20}$$

$$Hop(cm)(D) = 1.1\times10^{-4}\times D + 0.0055 \tag{21}$$

3) Frequency regime: 10^5 rad/s $< \omega$

$$Hop(cm)(T) = 4.9\times10^{-8}\times T^2 - 3.4\times10^{-5}\times T + 0.012 \tag{22}$$

$$Hop(cm)(D) = 3.1\times10^{-4}\times D + 0.0051 \tag{23}$$

The results through **Figure 8**, show that, regardless of the frequency range of modulation of the incident light, the optimum thickness decreases with temperature (Equations (18), (20) and (22)). The increase in the density of the photogenerated carriers with temperature causes the maximum density of the minority carriers to be reduced towards the junction (p/p^+) which is the illuminated surface [56]. Obtaining a large photocurrent then imposes a reduction in the thickness of the base. On the other hand, the increase in the diffusion coefficient of the minority charge carriers consequently leads to the increase in the optimum thickness (**Figure 9**), which is modeled by Equations (19), (21) and (23). The optimum thickness of the base is large at low frequencies corresponding to the static regime ($\omega\tau \ll 1$) whatever the temperature (**Figure 8**). In this interval of low frequencies, the relaxation time of the minority carriers is important (large values of D in Equation (5)), allowing a large distance of travel (Einstein relation). A large optimum thickness of the base is then obtained [43] [57] [58] (**Figure 9**). On the other hand, at high frequency values, the relaxation time ($\omega\tau \gg 1$) of minority carriers is reduced, as well as the coefficient (Equation (5)) and the scattering length (Equation (9)) of minorities corresponding to a short travel distance, then the optimum thickness [57] [58] of the base needed to collect the charge carriers is small, regardless of the temperature. Previous work on solar cells, monofacial, bifacial or multi-vertical junctions, corroborates these results, showing the reduction of the optimum thickness of the base of the silicon solar cell under illumination, according to the front (n^+) [34] [58] or rear (p^+) [38] [43] [57], while it is subjected to:

- Monochromatic light with constant flux [59] and absorption coefficient $\alpha(\lambda)$).
- Monochromatic light ($\alpha(\lambda)$) in frequency modulation (ω) [22] [23] [43] [57] [58].
- Constant B magnetic field [60] [61].

- Irradiation by charged particles [43] [62].
- Temperature variation [22] [63].
- Combination of several parameters leads to a situation of resonance of minority carriers' diffusion coefficient in the base of the solar cell under magnetic field:

1) In frequency [64].

2) In temperature, under front [36] [37], rear [39] [41], or vertical illumination [65].

3) And under irradiation of charged particles, in frequency [66].

4) Frequency and temperature [40] [42].

The analysis of the physical mechanisms [1] [24], through the phenomological parameters of the material [67], would lead to the development of optimized and economical solar cells [68] [69], taking into account above all the external physical factors, which constitute the operating environment.

5. Conclusions

The study of the density of the minority charge carriers in the base of the bifacial solar cell ($n^+/p/p^+$) silicon, under a given temperature and under monochromatic illumination in frequency modulation by the back side (p^+), showed the effect of the frequency, by the folding of the maximum density towards the junction (p/p^+) and the increase of the density of the photogenerated carriers with temperature. The graphic technique for the determination of the optimum thickness of the base of the bifacial solar cell ($n^+/p/p^+$) at temperature (T) and subjected to monochromatic illumination ($\alpha(\lambda)$) in frequency modulation (ω) by the back side, was used. The analysis of the dynamic photocurrent density curve as a function of the recombination velocity of minority carriers at junction (Sf), the dynamic recombination velocity expressions of minority carriers on the back side ($Sb(\alpha, H, D(\omega, T))$), and ($Sb(H, D(\omega, T)$) were deduced.

The graphical representation of the expressions of the dynamic recombination velocity of the minority carriers on the back side as a function of the thickness (H), made it possible to extract the base optimum thickness ($Hopt$), for each frequency domain and for different temperature values. The representation of the optimum thickness ($Hopt(T)$) gives a curve profile that is modeled by a function decreasing with temperature (T), regardless of the frequency of modulation of the incident light.

The variations of the dynamic coefficient ($D(\omega, T)$) of diffusion of the charge minorities are obtained by the variation of the frequency of modulation of the monochromatic light incident on the rear side (p^+). Thus the base optimum thickness *Hopt* decreases sharply with the frequency regime whatever the temperature (T).

Acknowledgements

In memory of the deceased professors emeritus, Professor Gerard W. COHEN

SOLAL (Montpellier University-France), Professor Michel RODOT (CNRS/ Meudon Bellevue, France), Professor Yembila Abdoulaye TOGUYENI and Professor Sié Faustin SIB, both at Joseph Ki ZERBO University (Ouagadougou, Burkina Faso).

Conflicts of Interest

The authors declare no conflicts of interest regarding the publication of this paper.

References

[1] Demesmaeker, E., Symons, J., Nijs, J. and Mertens, R. (1991) The Influence of Surface Recombination on the Limiting Efficiency and Optimum Thickness of Silicon Solar Cells. 10*th European Photovoltaic Solar Energy Conference*, Lisbon, 8-12 April 1991, 66-67. https://doi.org/10.1007/978-94-011-3622-8_17

[2] Sayem, A.A., Arafat, Y. and Rahman, M.M. (2014) Thickness Optimization and Composition Grading Effect in Heterojunction CIGS Solar Cell. 8*th International Conference on Electrical and Computer Engineering*, Dhaka, 20 December 2014, 524-527. https://doi.org/10.1109/ICECE.2014.7026952

[3] Yasar, S., Kahraman, S., Cetinkaya, S., Apaydin, S., Bilican, I. and Uluer, I. (2016) Numerical Thickness Optimization Study of CIGS Based Solar Cells with wxAMPS. *Optik*, **127**, 8827-8835. https://doi.org/10.1016/j.ijleo.2016.06.094

[4] Cuevas, A., Sinton, R.A. and King, R.R. (1991) A Technology-Based Comparison between Two-Sided and Back-Contact Silicon Solar Cells. *The* 10*th European Photovoltaic Solar Energy Conference*, Lisbon, 8-12 April 1991, 23-26. https://doi.org/10.1007/978-94-011-3622-8_6

[5] Meier, D.L., Hwang, J.M. and Campbell, R.B. (1988) The Effect of Doping Density and Injection Level on Minority Carrier Lifetime as Applied to Bifacial Dendritic Web Silicon Solar Cells. *IEEE Transactions on Electron Devices*, **35**, 70-79. https://doi.org/10.1109/16.2417

[6] Bordin, N., Kreinin, L. and Eisenberg, N. (2001) Determination of Recombination Parameters of Bifacial Silicon Cells with a Two Layer Step-Liked Effect Distribution in the Base Region. *Proceedings of the* 17*th European PVSEC*, Munich, 22-26 October 2001, 1495-1498.

[7] Sissoko, G., Correa, A., Nanema, E., Diarra, M.N., Ndiaye, A.L. and Adj, M. (1998) Recombination Parameters Measurement in Silicon Double Sided Surface Field Cell. *Proceeding of the World Renewable Energy Congress*, Florence, 20-25 September 1998, 1856-1859.

[8] Barro, F.I., Nanéma, E., Werème, A., Zougmoré, F. and Sissoko, G. (2001) Bulk and Surface Recombination Measurement in Silicon Double Sided Surface Field Solar Cell under Constant White Bias Illumination. *Proceedings of the* 17*th European Photovoltaic Solar Energy Conference*, Munich, 22-26 October 2001, 368-371.

[9] Green, M.A. and Keevers, M. (1995) Optical Properties of Intrinsic Silicon at 300K. *Progress in Photovoltaics*, **3**, 189-192. https://doi.org/10.1002/pip.4670030303

[10] Rajkanan, K., Singh, R. and Schewchun, J. (1979) Absorption Coefficient of Silicon for Solar Cell Calculations. *Solid-State Electronics*, **22**, 793-795. https://doi.org/10.1016/0038-1101(79)90128-X

[11] Sissoko, G., Sivoththanam, S., Rodo, M. and Mialhe, P. (1992) Constant Illumina-

tion-Induced Open Circuit Voltage Decay (CIOCVD) Method, as Applied to High Efficiency Si Solar Cells for Bulk and Back Surface Characterization. 11*th European Photovoltaic Solar Energy Conference and Exhibition*, Montreux, 12-16 October 1992, 352-354.

[12] Diallo, H.L., Maiga, A.S., Wereme, A. and Sissoko, G. (2008) New Approach of both Junction and Back Surface Recombination Velocities in a 3D Modelling Study of a Polycrystalline Silicon Solar Cell. *The European Physical Journal Applied Physics*, **42**, 193-211. https://doi.org/10.1051/epjap:2008085

[13] Diasse, O., Diao, A., Ly, I., Diouf, M.S., Diatta, I., Mane, R., Traore, Y. and Sissoko, G. (2018) Back Surface Recombination Velocity Modeling in White Biased Silicon Solar Cell under Steady State. *Journal of Modern Physics*, **9**, 189-201. https://doi.org/10.4236/jmp.2018.92012

[14] Diasse, O., Sam, R.S., Diallo, H.L., Ndiaye, M., Thiam, N., Mbodji, S. and Sissoko, G. (2012) Solar Cell's Classification by the Determination of the Specific Values of the Back Surface Recombination Velocities in Open Circuit and Short-Circuit Operating Conditions. *International Journal of Emerging Trends & Technology in Computer Science* (*IJETTCS*), **1**, 18-23.

[15] Joardar, K., Dondero, R.C. and Schroda, D.K. (1989) Critical Analysis of the Small-Signal Voltage-Decay Technique for Minority-Carrier Lifetime Measurement in Solar Cells. *Solid State Electronics*, **32**, 479-483. https://doi.org/10.1016/0038-1101(89)90030-0

[16] Zondervan, A., Verhoef, L.A. and Lindholm, F.A. (1988) Measurement Circuits for Silicon-Diode and Solar Cells Lifetime and Surface Recombination Velocity by Electrical Short-Circuit Current Delay. *IEEE Transactions on Electron Devices*, **35**, 85-88. https://doi.org/10.1109/16.2419

[17] Traore, Y., Thiam, N., Thiame, M., Thiam, A., Ba, M., Diouf, M., Diatta, I., Mballo, O., Sow, E., Wade, M. and Sissoko, G. (2019) AC Recombination Velocity in the Back Surface of a Lamella Silicon Solar Cell under Temperature. *Journal of Modern Physics*, **10**, 1235-1246. https://doi.org/10.4236/jmp.2019.1010082

[18] Gueye, M., Diallo, H., Moustapha, A., Traore, Y., Diatta, I. and Sissoko, G. (2018) Ac Recombination Velocity in a Lamella Silicon Solar Cell. *World Journal of Condensed Matter Physics*, **8**, 185-196. https://doi.org/10.4236/wjcmp.2018.84013

[19] Ly, I., Zerbo, I., Wade, M., Ndiaye, M., Dieng, A., Diao, A., Thiam, N., Thiam, A., Dione, M.M., Barro, F.I., Maiga, A.S. and Sissoko, G. (2021) Bifacial Silicon Solar Cell under Frequency Modulation and Monochromatic Illumination: Recombination Velocities and Associated Equivalent Electrical Circuits. *Proceedings of* 26*th European Photovoltaic Solar Energy Conference and Exhibition*, Hamburg, 5-9 September 2011, 298-301.

[20] Ly Diallo, H., Wade, M., Idrissa, L., Diaye, N.M., Dieng, B., Lemrabott, O.H., Amadou, S.M. and Sissoko, G. (2012) 1D Modeling of a Bifacial Silicon Solar Cell under Frequency Modulation, Monochromatic Illumination: Determination of the Equivalent Electrical Circuit Related to the Surface Recombination Velocity Research. *Journal of Applied Sciences, Engineering and Technology*, **4**, 1672-1676.

[21] Thiam, N., Diao, A., Ndiaye, M., Dieng, A., Thiam, A., Sarr, M., Maiga, A.S. and Sissoko, G. (2012) Electric Equivalent Models of Intrinsic Recombination Velocities of a Bifacial Silicon Solar Cell under Frequency Modulation and Magnetic Field Effect. Research *Journal of Applied Sciences, Engineering and Technology*, **4**, 4646-4655.

[22] Fall, M., Gaye, I., Diarisso, D., Diop, G., Loum, K., Diop, N., Sy, K., Ndiaye, M. and Sissoko, G. (2021) AC Back Surface Recombination Velocity in n^+-p-p^+ Silicon Solar

Cell under Monochromatic Light and Temperature. *Journal of Electromagnetic Analysis and Applications*, **13**, 67-81. https://doi.org/10.4236/jemaa.2021.135005

[23] Denise, K., Mamadou, L.B., Mamour, A.B., Gora, D., El Hadj, S., Oulimata, M. and Gregoire, S. (2020) AC Back Surface Recombination in n^+-p-p^+ Silicon Solar Cell: Effect of Temperature. *International Journal of Advanced Research* (*IJAR*), **8**, 140-151. https://doi.org/10.21474/IJAR01/11273

[24] Gaubas, E. and Vanhellemont, J. (1996) A Simple Technique for the Separation of Bulk and Surface Recombination Parameters in Silicon. *Journal of Applied Physics*, **80**, 6293-6297. https://doi.org/10.1063/1.363705

[25] Dorkel, J. and Leturcq, P. (1981) Carrier Mobilities in Silicon Solar Semi-Empirically Related Temperature, Doping and Injection Level. *Solid State Electron*, **24**, 821-825. https://doi.org/10.1016/0038-1101(81)90097-6

[26] Arora, N.D. and Hauser, J.R. (1982) Temperature Dependence of Silicon Solar Cell Characteristics. *Solar Energy Materials*, **6**, 151-158. https://doi.org/10.1016/0165-1633(82)90016-8

[27] Mane, R., *et al.* (2017) Minority Carrier Diffusion Coefficient D*(B, T): Study in Temperature on a Silicon Solar Cell under Magnetic Field. *Energy and Power Engineering*, **9**, 1-10. https://doi.org/10.4236/epe.2017.91001

[28] Diouf, S., Ndiaye, M., Thiam, N., Traore, Y., Ba, M., Diatta, I., Diouf, M., Mballo, O., Thiam, A., Ly, I. and Sissoko, G. (2019) Influence of Temperature and Frequency on Minority Carrier Diffusion Coefficient in a Silicon Solar Cell under Magnetic Field. *Energy and Power Engineering*, **11**, 355-361. https://doi.org/10.4236/epe.2019.1110023

[29] Dieng, A., Zerbo, I., Wade, M., Maiga, A.S. and Sissoko, G. (2011) Three-Dimensional Study of a Polycrystal Line Silicon Solar Cell: The Influence of the Applied Magnetic Field on the Electrical Parameters. *Semiconductor Science and Technology*, **26**, Article ID: 095023. https://doi.org/10.1088/0268-1242/26/9/095023

[30] Diao, A., Thiam, N., Zoungrana, M., Sahin, G., Ndiaye, M. and Sissoko, G. (2014) Diffusion Coefficient in Silicon Solar Cell with Applied Magnetic Field and under Frequency: Electric Equivalent Circuits. *World Journal of Condensed Matter Physics*, **4**, 84-92. https://doi.org/10.4236/wjcmp.2014.42013

[31] Wang, C.H. and Neugroschel, A. (1991) Minority-Carrier Lifetime and Surface Recombination Velocity Measurement by Frequency-Domain Photoluminescence. *IEEE Transactions on Electron Devices*, **38**, 2169-2180. https://doi.org/10.1109/16.83745

[32] Gupta, S., Ahmed, P. and Garg, S. (1988) A Method for the Determination of the Material parameters D, L, S and α from Measured Short-Circuit Photocurrent. *Solar Cells*, **25**, 61-72. https://doi.org/10.1016/0379-6787(88)90058-0

[33] Mandelis, A. (1989) Coupled ac Photocurrent and Photothermal Reflectance Response Theory of Semiconducting p-n Junctions. I. *Journal of Applied Physics*, **66**, 5572-5583. https://doi.org/10.1063/1.343662

[34] Maimouna Mint, E.L.Y., Thiam, N., Ndiaye, M., Traore, Y., Mane, R., El hadji, S., Mballo, O., Dieng, M.S., Sarr, C.T., Ly, I. and Sissoko, G. (2020) Surface Recombination Velocity Concept as Applied to Determinate Back Surface Illuminated Silicon Solar Cell Base Optimum Thickness, under Temperature and External Magnetic Field Effects. *Journal of Scientific and Engineering Research*, **7**, 69-77. http://www.jsaer.com

[35] Sall, M., Fall, M.F.M., Diasse, O., *et al.* (2022) Determination of Optimum Thickness of the Base of n^+/p/p^+ Silicon Solar Cell, Illuminated by the Rear Face by a

Monochromatic Light of Long Wavelength in Frequency Modulation. *Journal of Chemical, Biological and Physical Sciences*, **11**, 64-77.

[36] Diagne, S., Sow, O., Diop, G., *et al.* (2022) Optimization of Silicon Solar Cell Base Thickness, While Illuminated by a Long Wavelength Monochromatic Light: Influence of both Lorentz Law and Umclapp Process. *International Journal of Advanced Research*, **10**, 133-143. https://doi.org/10.21474/IJAR01/15158

[37] Diagne, S., Diop, G., Mane, R., *et al.* (2022) Monochromatic Ligth of Short Wavelength as Applied to Determine ($n^+/p/p^+$) Silicon Solar Cell Base Thickness under the Influence of both Magnetic Field and Temperature. *International Journal of Engineering Research Updates*, **3**, 13-25. https://doi.org/10.53430/ijeru.2022.3.2.0055

[38] Dione, G.N., Ba, H.Y., Diop, G., *et al.* (2022) Bifacial (n^+-p-p^+) Silicon Solar Cell base Thickness Optimization, While Illuminated by the Rear Face with Monochromatic Light of Short Wavelenths. *International Journal of Advanced Research* (*IJAR*), **10**, 409-418. https://doi.org/10.21474/IJAR01/15372

[39] Diop, M., Ba, H., Thiam, N., Diatta, I., Traore, Y., Ba, M., Sow, E., Mballo, O. and Sissoko, G. (2019) Surface Recombination Concept as Applied to Determinate Silicon Solar Cell Base Optimum Thickness with Doping Level Effect. *World Journal of Condensed Matter Physics*, **9**, 102-111. https://doi.org/10.4236/wjcmp.2019.94008

[40] Sow, O., Gueye, S., Mane, R., *et al.* (2022) ($n^+/p/p^+$) Silicon Solar Cell Base Thickness Optimization under Modulated Short Wavelength Illumination, at Resonances in both Frequency and Temperature of Minority Carriers Diffusion Coefficient. *International Journal of Engineering Research Updates*, **3**, 40-52. https://doi.org/10.53430/ijeru.2022.3.2.0059

[41] Diop, A., Mane, R., Diop, G., *et al.* (2022) Bifacial Silicon ($n^+/p/p^+$) Silicon Solar Cell Base Thickness Optimization under Back Illumination of Long Wavelengh: Effect of Diffusion Coefficient Resonance in Temperature under Applied Magnetic Field. *Journal of Scientific and Engineering Research*, **9**, 152-165. http://www.jsaer.com

[42] Diop, G., Sow, O., Thiame, M., Mane, R., Diatta, I., Loum, K., Gueye, S., Wade, M. and Sissoko, G. (2022) Diffusion Coefficient at Double Resonances in Frequency and Temperature, Applied to ($n^+/p/p^+$) Silicon Solar Cell Base Thickness Optimization under Long Wavelength Illumination. *Journal of Electromagnetic Analysis and Applications*, **14**, 89-103. https://doi.org/10.4236/jemaa.2022.148008

[43] Ndiaye, M., Sow, O., Diatta, I., *et al.* (2022) Optimization of the Thickness of the Doping Rate Base (Nb) of the ($n^+/p/p^+$) Silicon Solar Cell with Vertical Multi-Junction Connected in Series and Placed under Monochromatic Illumination in Frequency Modulation. *Journal of Chemical, Biological and Physical Sciences*, **12**, 266-280. https://doi.org/10.24214/jcbps.C.12.4.25165

[44] Gning, A.S., Ba, M.L., Ba, M.A., *et al.* (2020) Optimum Base Thickness Determination of a Back Illuminated Silicon Solar Cell: Irradiation Effect. *International Journal of Advanced Research*, **8**, 100-109. https://doi.org/10.21474/IJAR01/11268

[45] Kunst, M. and Sanders, A. (1992) Transport of Excess Carriers in Silicon Wafers. *Semiconductor Science and Technology*, **7**, 51-59. https://doi.org/10.1088/0268-1242/7/1/009

[46] De Vischere, P. (1986) Comment on G.J. Rees "Surface Recombination Velocity—A Useful Concept". *Solid-State Electronics*, **29**, 1161-1165. https://doi.org/10.1016/0038-1101(86)90059-6

[47] Sy, K.M., Diene, A., Tamba, S., *et al.* (2016) Effect of Temperature on Transient Decay Induced by Charge Removal of a Silicon Solar Cell under Constant Illumination. *Journal of Scientific and Engineering Research*, **3**, 433-445. https://www.jsaer.com

[48] Sylla, B., Ly, I., Sow, O., Dione, B., Traore, Y. and Sissoko, G. (2018) Junction Surface Recombination Concept as Applied to Silicon Solar Cell Maximum Power Point Determination Using Matlab/Simulink: Effect of Temperature. *Journal of Modern Physics*, **9**, 172-188. https://doi.org/10.4236/jmp.2018.92011

[49] Sissoko, G., Nanéma, E., Corréa, A., Biteye, P.M., Adj, M. and N'Diaye, A.L. (1998) Silicon Solar Cell Recombination Parameters Determination Using the Illuminated I-V Characteristic. *World Renewable Energy Congress*, Florence, 20-25 September 1998, 1847-1851.

[50] Ndiaye, E.H., Sahin, G., Thiam, A., Dieng, M., Diallo, H.L., Ndiaye, M. and Sissoko, G. (2015) Study of the Intrinsic Recombination Velocity at the Junction of Silicon Solar under Frequency Modulation and Irradiation. *Journal of Applied Mathematics and Physics*, **3**, 1522-1535. https://doi.org/10.4236/jamp.2015.311177

[51] Le Quang, N., Rodot, M., Ghannam, M., Coppye, J., *et al.* (1992) Solar Cells with 15.6% Efficiency on Multicrystalline Silicon, Using Impurity Gettering, Back Surface Field and Emitter Passivation. *International Journal of Solar Energy*, **11**, 273-279. https://doi.org/10.1080/01425919208909745

[52] Fossum, J.G. (1977) Physical Operation of Back-Surface-Field Silicon Solar Cells. *IEEE Transactions on Electron Devices*, **2**, 322-325. https://doi.org/10.1109/T-ED.1977.18735

[53] Tall, I., Seibou, B., El Moujtaba, M.A.O., Diao, A., *et al.* (2015) Diffusion Coefficient Modeling of a Silicon Solar Cell under Irradiation Effect in Frequency: Electric Equivalent Circuit. *International Journal of Engineering Trends and Technology* (*IJETT*), **19**, 56-61. https://www.ijettjournal.org https://doi.org/10.14445/22315381/IJETT-V19P211

[54] Zerbo, I., Barro, F.I., Mbow, B., Diao, A., Madougou, S., Zougmore, F. and Sissoko, G. (2004) Theoretical Study of Bifacial Silicon Solar Cell under Frequency Modulate white Light: Determination of Recombination Parameters. *Proceedings of the* 19*th European Photovoltaic Solar Energy Conference*, Paris, 7-11 June 2004, 258-261.

[55] Ly, I., Ndiaye, M., Wade, M., Thiam, N., Gueye, S. and Sissoko, G. (2013) Concept of Recombination Velocity Sfcc at the Junction of a Bifacial Silicon Solar Cell, in Steady State, Initiating the Short-Circuit Condition. *Research Journal of Applied Sciences, Engineering and Technology*, **5**, 203-208. https://doi.org/10.14445/22315381/IJETT-V19P211

[56] Diatta, I., Ly, I., Wade, M., Diouf, M.S., Mbodji, S. and Sissoko, G. (2016) Temperature Effect on Capacitance of a Silicon Solar Cell under Constant White Biased Light. *World Journal of Condensed Matter Physics*, **6**, 261-268. https://doi.org/10.4236/wjcmp.2016.63024

[57] Sall, M., Diarisso, D., Faty Mbaye Fall, M., Diop, G., Ndiaye, M., Loum, K. and Sissoko, G. (2021) Back Illuminated N/P/P$^+$ Bifacial Silicon Solar Cell under Modulated Short-Wavelength: Determination of Base Optimum Thickness. *Energy and Power Engineering*, **13**, 207-220. https://doi.org/10.4236/epe.2021.135014

[58] Ndiaye, A., Gueye, S., Sow, O., *et al.* (2020) A.C. Recombination Velocity as Applied to Determine n$^+$/p/p$^+$ Silicon Solar Cell Base Optimum Thickness. *Energy and Power Engineering*, **12**, 543-554. https://doi.org/10.4236/epe.2020.1210033

[59] Dede, M.M.S., Ba, M.L., Ba, M.A., Ndiaye, M., Gueye, S., Sow, E.H., Diatta, I., Diop, M.S., Wade, M. and Sissoko, G. (2020) Back Surface Recombination Velocity Dependent of Absorption Coefficient as Applied to Determine Base Optimum Thickness of an n$^+$/p/p$^+$ Silicon Solar Cell. *Energy and Power Engineering*, **12**, 445-458. https://doi.org/10.4236/epe.2020.127027

[60] Thiaw, C., Ba, M., Amadou Ba, M., *et al.* (2020) n^+-p-p^+ Silicon Solar Cell Base Optimum Thickness Determination under Magnetic Field. *Journal of Electromagnetic Analysis and Applications*, **12**, 103-113. https://doi.org/10.4236/jemaa.2020.127009

[61] Diop, G., Ba, H.Y., Thiam, N., *et al.* (2019) Base Thickness Optimization of a Vertical Series Junction Silicon Solar Cell under Magnetic Field by the Concept of Back Surface Recombination Velocity of Minority Carrier. *ARPN Journal of Engineering and Applied Sciences*, **14**, 4078-4085.

[62] Ba, M.L., Thiam, N., Thiame, M., *et al.* (2019) Base Thickness Optimization of a (n^+-p-p^+) Silicon Solar Cell in Static Mode under Irradiation of Charged Particles. *Journal of Electromagnetic Analysis and Applications*, **11**, 173-185. https://doi.org/10.4236/jemaa.2019.1110012

[63] Ndiaye, F.M., Ba, M.L., Ba, M.A., Diop, G., Diatta, I., Sow, E.H., Mballo, O. and Sissoko, G. (2020) Lamella Silicon Optimum Width Determination under Temperature. *International Journal of Advanced Research*, **8**, 1409-1419. https://doi.org/10.21474/IJAR01/11228

[64] Ndiaye, A., Gueye, S., Mbaye Fall, M., Diop, G., Ba, A., Ba, M., Diatta, I., Habiboullah, L. and Sissoko, G. (2020) Diffusion Coefficient at Resonance Frequency as Applied to n^+/p/p^+ Silicon Solar Cell Optimum Base Thickness Determination. *Journal of Electromagnetic Analysis and Applications*, **12**, 145-158. https://doi.org/10.4236/jemaa.2020.1210012

[65] Faye, D., Gueye, S., Ndiaye, M., *et al.* (2020) Lamella Silicon Solar Cell under both Temperature and Magnetic Field: Width Optimum Determination. *Journal of Electromagnetic Analysis and Applications*, **12**, 43-55. https://doi.org/10.4236/jemaa.2020.124005

[66] Sarr, M., Gaye, I., Ndiaye, S.A., Lamine, M., Diop, G., *et al.* (2021) Effet de l'irradiation par des particules chargees sur le coefficient de diffusion de la base d'une photopile au silicium (n^+-p-p^+): Determination de l'epaisseur optimum sous eclairement monochromatique. *International Journal of Advanced Research*, **9**, 127-135. https://doi.org/10.21474/IJAR01/12565

[67] Navruz, T.S. and Saritas, M. (2012) Determination of the Optimum Material Parameters for Intermediate Band Solar Cells Diffusion Model. *Progress in Photovoltaics Research and Applications*, **22**, 593-602. https://doi.org/10.1002/pip.2283

[68] Lago-Aurrekoetxea, R.M., *et al.* (2001) Fabrication Process for Thin Silicon Solar Cells. *Proceedings* 17*th European PVSEC*, Munich, 22-26, October 2001, 1519-1522.

[69] Sun, X., Khan, M.R., Deline, C. and Alam, M.A. (2018) Optimization and Performance of Bifacial Solar Modules: A Global Perspective. *Applied Energy*, **212**, 1601-1610. https://doi.org/10.1016/j.apenergy.2017.12.041